Iranian Journal of Fuzzy Systems

Volume 16, Number 1, (2019), pp. 33-48

University of Sistan and Baluchestan

Multimodal medical image fusion based on yager's intuitionistic fuzzy sets

T. Tirupal[1], B. Chandra Mohan[2] and S. Srinivas Kumar[3]

[1] *Research Scholar, Department of ECE JNTUK, Kakinada, Andhra Pradesh, India*
[2] *Professor & Head of ECE Bapatla Engineering College Bapatla, Andhra Pradesh, India*
[3] *Professor of ECE & Director (R&D) JNTUK, Kakinada Andhra Pradesh, India*

tirutalari@gmail.com, chandrabhuma@gmail.com, samay_ssk2@yahoo.com

Abstract

The objective of image fusion for medical images is to combine multiple images obtained from various sources into a single image suitable for better diagnosis. Most of the state-of-the-art image fusing technique is based on non-fuzzy sets, and the fused image so obtained lags with complementary information. Intuitionistic fuzzy sets (IFS) are determined to be more suitable for civilian, and medical image processing as more uncertainties are considered compared with fuzzy set theory. In this paper, an algorithm for effectively fusing multimodal medical images is presented. In the proposed method, images are initially converted into Yager's intuitionistic fuzzy complement images (YIFCIs), and a new objective function called intuitionistic fuzzy entropy (IFE) is employed to obtain the optimum value of the parameter in membership and non-membership functions. Next, the YIFCIs are compared using contrast visibility (CV) to construct a decision map (DM). DM is refined with consistency verification to create a fused image. Simulations on several pairs of multimodal medical images are performed and compared with the existing fusion methods, such as simple average, discrete cosine transform (DCT), redundant wavelet transform (RWT), intuitionistic fuzzy set, fuzzy transform and interval-valued intuitionistic fuzzy set (IVIFS). The superiority of the proposed method is presented and is justified. Fused image quality is also verified with various quality metrics, such as spatial frequency (SF), average gradient (AG), fusion symmetry (FS), edge information preservation ($Q^{AB/F}$), entropy (E) and computation time (CoT).

Keywords: Image fusion, Intuitionistic fuzzy sets, Multimodal medical images, Intuitionistic fuzzy entropy, Decision map.

1 Introductions

Medical images provide different types of information: CT (computed tomography) images embed with less distortion and provide details regarding dense structures, such as bones, MRI (magnetic resonance imaging) provide information about pathological soft tissues, MRA (magnetic resonance angiography) easily detects abnormalities in the brain, X-ray detects fractures and abnormalities in bone positions, VA (vibro-acoustography), provide the depth and thickness of the disease object, and PET (positron emission tomography) and SPECT (single photon emission computed tomography) provide functional and metabolic data about the human brain. By combining these in multimodal medical image pairs such as CT-MRI [27], MRI-MRA, Xray-VA [18], MRI-PET [6], and MRI-SPECT, additional clinical information can be extracted that is complimentary in nature. Therefore, we can say that a single image will provide all relevant information, and hence multimodal medical image fusion is necessarily required to obtain all possible information in a single composite image called a fused image. Multimodal medical image fusion [12, 31] is the process of combining two multimodal medical images to increase the quality of the output image. Its benefits include the extended range

Corresponding Author: T. Tirupal
Received: June 2017; Revised: August 2017; Accepted: April 2018.

of operation, reduced uncertainty, robust system performance, improved consistency and squashed demonstration of information for better treatment and precise diagnosis. A detailed survey of medical image fusion techniques can be found in [20]. Some multimodal medical image fusion applications include detection of brain tumors [14], breast cancer assessment [33], oncology, ultrasound [21] and diagnosis of cardiac diseases [8].

Image fusion techniques are characterized based on the level of processing and based on the acquisition of images. The level of processing is categorized into four classes, namely, pixel level fusion [23], which includes basic arithmetic, probabilistic and logical operations, which directly combine the pixel values of two images to be fused but reduce feature contrast. In block-level fusion [1], the images are divided into blocks, and the one with more perceptibility is transferred to a fused image, but this presents blocking artifacts in the fused image that are undesired. In feature-level fusion, the extraction of such features as contrast, texture, shape and size are included in the fusion performance, whereas in decision-level fusion, a mixture of multiple algorithms is involved to obtain the ultimate fused image, but this fusion level hazes the harsh edges.

2 Literature Review

Image fusion finds applications in the military, remote sensing, robots, security, surveillance and medical diagnosis. The most important research issue is to extract the maximum amount of information by fusing multi-resolution images. Various techniques include pixel averaging [27], which is the modest image fusion technique and takes a pixel-by-pixel average of the two images but clues to adverse side effects, such as contrast reduction. Principal Component Analysis (PCA) depends on the principal components of the image and Intensity-Hue-Saturation (IHS) [17]. However, PCA and IHS show the degraded performance of the fused image. Moment [32] based fusion is unable to detect the edges clearly, and the Singular Value Decomposition (SVD) [25] and Discrete Cosine Transform (DCT) [16] method are more appropriate for present applications and provide a better quality of the fused image, but these methods are weak in terms of boundary detection of a disease (in a medical image) present in the fused image. Discrete Cosine Harmonic Wavelet Transform (DCHWT) [29] reduces computational complication, but the quality of the image is poor because of uncertainties present in the image. Multi-resolution techniques, such as wavelet transforms [35], preserve different frequency information in a stable form and allow for good localization in the time and frequency domain, but the major drawback is that they do not provide shift invariance in the coefficients. This problem can be overcome by using a Redundant Wavelet Transform (RWT) [22].The major drawback of RWT is increased computational complexity as the wavelet is undecimated. Shift invariance is more desirable and is successfully applied in various phases of image processing, such as image enhancement, image fusion and image de-noising, and this can be observed more in Non-Subsampled Contourlet Transform (NSCT) [7].

Fuzzy set theory theatres a vital role in the image processing proposed by Zadeh [39] to remove the ambiguity and vagueness present in images. Fuzzy sets by Zadeh can practice imperfect data if this imperfection originates from haziness and obscurity rather than randomness. Fuzzy sets in image processing increase contrast, flat the regions of interest, and refine the edges and fine erections of the image. Fuzzy sets use the membership function to remove the vagueness present in the image. While describing the membership function, an uncertainty due to lack of knowledge or personal error is found, which primes to another uncertainty called hesitation degree. The combination of membership, non-membership, and hesitation degree defines the intuitionistic fuzzy set introduced by Atanassov [3] in 1986. Medical images are poorly illuminated, contain many uncertainties in the form of noise, have vague boundaries, have overlapping gray levels, have invisible blood vessels, and it is difficult to extract objects from the image. These problems can be solved by considering IFS. In the proposed method, an intuitionistic fuzzy set called the Yager's intuitionistic fuzzy complement set [34] is used to eliminate the uncertainties present in multimodal medical images. Many uncertainties exist in every phase of image processing, and in using IFS [5] and fuzzy transforms [26], these uncertainties can be removed, and the image is enhanced regarding the contrast of the image.

This paper proposes a different method for merging two or more images using Yager's intuitionistic fuzzy complement sets. In the proposed method, initially, the registered [15] source images are fuzzified, and then the finest value of the bound is calculated for membership, non-membership and hesitation degree by means of IFE [11] and is also compared with Yue entropy [38]. Then, Yager's intuitionistic fuzzy complement images are generated for source images, and a decision map is constructed using the contrast visibility of YIFCIs. The DM is then refined with a consistency verification to generate a fused image without uncertainty. The fused image is then defuzzified to obtain a crisp image without uncertainty. The proposed method is also compared with IVIFS method.

3 Intuitionistic Fuzzy Approach to Image Fusion

3.1 Intuitionistic Fuzzy Set:

Image processing by intuitionistic fuzzy sets mainly requires membership and non-membership functions. The construction of IFS is briefly explained when initiating from fuzzy sets. A fuzzy set Z in a finite set Y=$\{y_1, y_2, y_3, ..., y_n\}$ may be mathematically denoted as:

$$Z = \{(y, \mu_Z(y))|y \in Y\} \tag{1}$$

Where the function $\mu_Z(y) : Y \to [0, 1]$ denotes the membership degree of an element y in the finite set Y. Then, the non-membership degree will be $1 - \mu_Z(y)$.

Atanassov introduced a new fuzzy set called the intuitionistic fuzzy set, which takes both membership $\mu(y)$ and non-membership $v(y)$ into consideration, holding $\mu_Z(y) \to [0, 1]$, $v_Z(y) \to [0, 1]$. An intuitionistic fuzzy set Z in y is inscribed as:

$$Z = \{(y, \mu_Z(y), v_Z(y))|y \in Y\} \tag{2}$$

Which holds the condition $0 \leq \mu_Z(y) + v_Z(y) \leq 1$. A new parameter $\Pi_Z(y)$ called the hesitation degree presented by Szmidt and Kacpryzk [30] ascends due to absence of knowledge while describing the membership degree, for each component y in Z is given by:

$$\Pi_Z(y) = 1 - \mu_Z(y) - v_Z(y) \tag{3}$$

Where $0 \leq \Pi_Z(y) \leq 1$. Based on the hesitation degree, the intuitionistic fuzzy set is defined as

$$Z = \{(y, \mu_Z(y), v_Z(y), \Pi_Z(y))|y \in Y\} \tag{4}$$

3.2 Interval-Valued Intuitionistic Fuzzy Set:

Atanassov and Gargov [4] extended the intuitionistic fuzzy set to the interval-valued intuitionistic fuzzy set (IVIFS), which is described by a membership function and a non-membership function whose values are intervals rather than real numbers. This approach not only expands the ability of the intuitionistic fuzzy set to handle uncertain information but also improves its ability to solve practical decision-making problems. The notion of IVIFS is as follows:

Let $\mu_Z(y) = [\mu_Z^-(y), \mu_Z^+(y)]$ and $v_Z(y) = [v_Z^-(y), v_Z^+(y)]$ are intervals, $\mu_Z^-(y) = inf\mu_Z(y), \mu_Z^+(y) = sup\mu_Z(y), v_Z^-(y) = inf v_Z(y), v_Z^+(y) = sup v_Z(y)$, then

$$Z^{IVIFS} = \{y, [\mu_Z^-(y), \mu_Z^+(y)], [v_Z^-(y), v_Z^+(y)]|y \in Y\} \tag{5}$$

with $0 \leq \mu_Z^+(y) + v_Z^+(y) \leq 1$. The hesitation degree also lie in an interval which is given as

$$\Pi_Z(y) = [\Pi_Z^-(y), \Pi_Z^+(y)] = [1 - \mu_Z^-(y) - v_Z^-(y), 1 - \mu_Z^+(y) - v_Z^+(y)] \tag{6}$$

If $\mu_Z(y) = \mu_Z^-(y) = \mu_Z^+(y)$ and $v_Z(y) = v_Z^-(y) = v_Z^+(y)$, then IVIFS becomes IFS. After the pioneering work of Atanassov and Gargov, the IVIFS has received much attention from researchers [36, 37]. Finally, an interval-valued intuitionistic fuzzy set image (IVIFSI) is molded as:

$$F^{IVIFSI} = \{y, [\mu_Z^-(y), \mu_Z^+(y)], [v_Z^-(y), v_Z^+(y)], [\Pi_Z^-(y), \Pi_Z^+(y)]|y \in Y\} \tag{7}$$

3.3 Yager's Intuitionistic Fuzzy Complement Set:

A function $\phi(y)$ is called an intuitionistic fuzzy generator [10] if: $\phi(y) \leq (1-y)$ for all $y \in [0,1]$. From Yager generating function [13], an intuitionistic fuzzy generator or fuzzy supplement is generated, and the fuzzy supplement function is well-defined as:

$$N(\mu(y)) = g^{-1}(g(1) - g(\mu(y))) \tag{8}$$

Where $g(\cdot)$ is an aggregate function, and $g : [0,1] \to [0,1]$. Using the subsequent function in the overhead equation (8), Yager class can be generated

$$g(y) = y^{\alpha} \tag{9}$$

Now, Yager's intuitionistic fuzzy complement is inscribed as:

$$N(y) = (1 - y^{\alpha})^{1/\alpha} \tag{10}$$

where $\alpha > 0$ and $N(1) = 0$, $N(0) = 1$. From the function $N(y)$, non-membership standards are designed and the Yager's intuitionistic fuzzy complement set (YIFCS) becomes:

$$Z_{\alpha}^{YIFCS} = \{y, \mu_Z(y), (1 - \mu_Z(y)^{\alpha})^{1/\alpha} | y \in Y\} \tag{11}$$

and the hesitation degree is given as:

$$\Pi_Z(y) = 1 - \mu_Z(y) - (1 - \mu_Z(y)^{\alpha})^{1/\alpha} \tag{12}$$

By varying the α parameter, we can obtain different Yager's intuitionistic fuzzy complement sets. As α is not fixed for all the images, the optimum value of α is obtained using IFE.

3.4 Intuitionistic Fuzzy Entropy:

3.4.1 Chaira's IFE [11]:

Entropy theatres a significant part in image processing, and fuzzy entropy measures fuzziness in a fuzzy set. The notion of fuzzy entropy was first introduced by Zadeh in 1969, and the skeleton of non-probabilistic entropy was introduced first by De Luca and Termini [13]; many authors [9] have since suggested different types of entropy methods by means of intuitionistic fuzzy set theory. In this work, a new objective function called IFE is introduced, can be computed as in [11] and has been used to advance the proposed scheme, which is designated as

$$IFE(Z;\alpha) = \sum_{i=1}^{n} \Pi_Z(y_i) exp(1 - \Pi_Z(y_i)) \tag{13}$$

Where $\Pi_Z(y_i) = 1 - (\mu_Z(y_i) + v_Z(y_i))$ is the hesitation degree, $\mu_Z(y_i)$ is the membership function and $v_Z(y_i)$ is the non-membership function. Entropy (IFE) is calculated using equation (13) for α values ranging from [0.1, 1], and it is optimized by finding the maximum entropy value, that is

$$\alpha_{opt} = argmax(IFE(Z;\alpha)) \tag{14}$$

Using this known value of α, the membership degrees of the pixels in the YIFCIs are designed, and finally, a YIFCI is molded as below.

$$F_{YIFCI} = \{(y, \mu_Z(y), v_Z(y;\alpha), \Pi_Z(y;\alpha)) | y \to Y\} \tag{15}$$

3.4.2 Yue Entropy [38]:

The degree of fuzziness of a fuzzy set can be measured by defining different magnitudes of a fuzzy set. The same thing is done for IFSs, that is, the degree of intuitionism of an intuitionistic fuzzy set is measured by defining different magnitudes of IFSs. From this idea the intuitionistic entropy [38] is defined as:

$$E_\alpha = -\frac{1}{ln(mn)} \sum_{i=1}^{m} \sum_{j=1}^{n} P_{ij}^{\alpha} ln P_{ij}^{\alpha} \tag{16}$$

$\alpha \in T(1, 2, ..., t)$ where $P_{ij}^{\alpha} = \dfrac{\Pi_{ij}^{\alpha}}{\sum_{i=1}^{m} \sum_{j=1}^{n} \Pi_{ij}^{\alpha}}$

4 Proposed Method for Medical Image Fusion

This section addresses a proposed system for multimodal medical image fusion using YIFCS and contrast visibility.

4.1 Contrast Visibility:

Contrast visibility defines the amount of deviation of pixels in an image block from the mean value of the block. It discourses the lucidity of the consistent blocks. The contrast visibility of the image block is calculated by means of equation (13) and can be observed in [1].

$$CV = \frac{1}{p \times q} \sum_{(i,j) \in B_k} \frac{|I(i,j) - \mu_k|}{\mu_k} \tag{17}$$

Where μ_k and $p \times q$ are the mean and magnitude of the block B_k, respectively.

4.2 Proposed Algorithm:

The proposed multimodal medical image fusion based on Yager's intuitionistic fuzzy complement set is demonstrated in Figure 1, and the fusion procedure is accomplished by the subsequent steps:
1. Read the two input source images and denote as I_1 and I_2.
2. The first image I_1 of size $M \times N$ is fuzzified by means of the formula

$$\mu_{Z1}(I_{ij1}) = \frac{I_{ij1} - l_{min}}{l_{max} - l_{min}} \tag{18}$$

Where I_{ij1} defines the gray level of the first image and ranges from 0 to $L-1$ (L is the extreme gray level value). l_{min} and l_{max} represent the least and extreme gray level values of the first image.
3. Calculate the optimum value of α using entropy equations (13) & (14) for the first image and this α varies for different input images. α is also varied for Entropy equations of Yue [38] and the output images are compared.
4. With the optimum value of α, find fuzzified YIFCI for the first input image by using below equations and denote as I_{Y1}.

$$\mu_{YIFCS1}(I_{ij1}) = \mu_{Z1}(I_{ij1}) \tag{19}$$

$$v_{YIFCS1}(I_{ij1}; \alpha) = (1 - \mu_{YIFCS1}(I_{ij1})^{\alpha})^{1/\alpha} \tag{20}$$

$$\Pi_{YIFCS1}(I_{ij1}; \alpha) = (1 - \mu_{YIFCS1}(I_{ij1}) - v_{YIFCS1}(I_{ij1}; \alpha) \tag{21}$$

$$I_{Y1} = \{\mu_{YIFCS1}(I_{ij1}), v_{YIFCS1}(I_{ij1}; \alpha), \Pi_{YIFCS1}(I_{ij1}; \alpha)\} \tag{22}$$

5. Repeat the above procedure from step 2 to step 4 for the second input image to find YIFCI, I_{Y2}.

$$I_{Y2} = \{\mu_{YIFCS2}(I_{ij2}), v_{YIFCS2}(I_{ij2}; \alpha), \Pi_{YIFCS2}(I_{ij2}; \alpha)\}$$

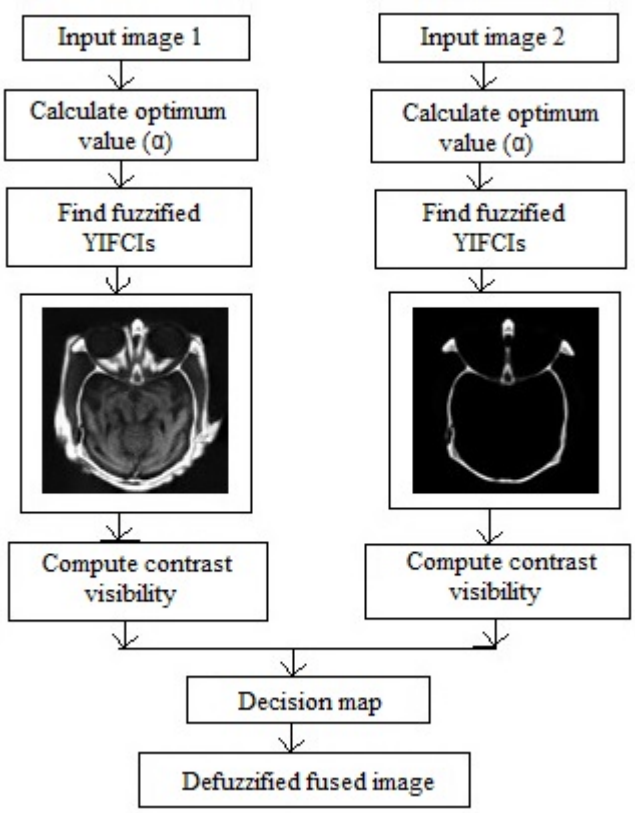

Figure 1: Block diagram of proposed method

(23)

6. Decompose the two images I_{Y1} and I_{Y2} into $m \times n$ windows–the size of each window is taken as 5×5 in this paper– and then compute the contrast visibility (CV) of each window separately. Then, a decision map (DM) is constructed that determines the combination of pixels of the two images.

$$DM = \begin{cases} 1 & \text{if } CV_i^{I_{Y1}} > CV_i^{I_{Y2}} \\ -1 & \text{if } CV_i^{I_{Y1}} < CV_i^{I_{Y2}} \\ 0 & \text{if } CV_i^{I_{Y1}} = CV_i^{I_{Y2}} \end{cases} \tag{24}$$

$CV_i^{I_{Y1}}$ and $CV_i^{I_{Y2}}$ are the contrast visibilities of the ith window of images I_{Y1} and I_{Y2} respectively. DM is the decision map built by taking the decision for each coefficient using the contrast visibility of respective window.
7. DM is refined with consistency verification using the majority filter introduced by Li et al. [24] to create a new decision map (NDM).
8. The fused image (FI) without uncertainty is attained based on the NDM as

$$FI(i,j) = \begin{cases} I_{Y1}(i,j) & \text{if } NDM(i,j) = 1 \\ I_{Y2}(i,j) & \text{if } NDM(i,j) = -1 \\ [I_{Y1}(i,j) + I_{Y2}(i,j)]/2 & \text{if } NDM(i,j) = 0 \end{cases} \tag{25}$$

9. Finally, the fused image is defuzzified to obtain a crisp image using the defuzzification equation obtained by the inverse of equation (18)

$$I'(i,j) = (l_{max} - l_{min}) * \mu_{YIFCS}(FI(i,j)) + l_{min} \tag{26}$$

Where l_{min} and l_{max} in the above equation represent the lowest and extreme gray level values of the fused image FI.

Fusion Method	SD	AG	E	FS	CC	SF	$Q^{AB/F}$	CoT
Naidu et al.[28]	40.06	9.504	6.003	1.674	0.674	24.33	0.568	2.30
Haghighat et al.[16]	63.09	15.70	6.801	1.666	0.630	32.28	0.830	3.08
Li et al.[22]	63.02	15.99	6.819	1.659	0.633	32.44	0.866	7.25
Bala et al.[5]	69.28	14.43	5.357	1.699	0.665	30.78	0.752	3.95
Meenu et al.[26]	61.88	14.46	6.782	1.635	0.600	31.51	0.732	2.76
Proposed method	81.66	16.43	6.806	1.642	0.647	32.23	0.636	3.75
IVIFS method	59.42	12.56	6.503	1.644	0.655	25.17	0.745	3.1

Table 1: Objective evaluation of different image fusion methods with proposed Yager's intuitionistic fuzzy complement set method for Figure 2

5 Experimental Results

Based on the proposed algorithm, simulations are carried out in different sets of medical images, and the details are presented in this section. In this work, all the source images are assumed to be properly registered. The first example shown in Figure 2 discourses CT and MRI images (available in www.metapix.de/toolbox.htm) that are complementary in nature, with a size of . The CT image provide information about bones and hard tissues while the MRI image gives soft tissue information. Fusing these two images provide abundant information in a single image, which helps to better diagnose a disease. Figure 2(H) is the fusion result of the proposed method, which visually proves that the image is of higher contrast and luminance than the fused image of existing methods, such as Simple average [28], DCT [16], RWT [22], intuitionistic fuzzy set [5] and Fuzzy transform [26].

Further comparisons of the results are performed using few objective criteria used in [19], such as standard deviation (SD) measured in pixel intensity, the average gradient (AG) measured as change in intensity per pixel, entropy (E) measured in bits per pixel, fusion symmetry (FS), correlation coefficient (CC), spatial frequency (SF) measured in cycles per millimeter, edge strength preservation ($Q^{AB/F}$) and computation time (CoT) measured in seconds, and the results are listed in Table 1. It is observed from the table that the proposed method provide better performance regarding contrast, luminance, and visibility of the fused image. Figures 2(K-R) show magnified results of existing and proposed methods which prove that fused image has fine edges and sharp features. The proposed method is also compared with IVIFS [36] and the fused image in Figure 2(I) represents that the features are more enhanced with less computation time of 3.1 seconds than the other methods. It is also found from Table 1 that the Fusion Symmetry (FS) and edge information preservation ($Q^{AB/F}$) are more compared to proposed method. The fused image for Yue entropy [38] can also be seen in Figure 2(J) and we can say that the output image is not much enhanced than that of the other methods.

The second example addresses a T1-weighted MR image and MRA image with some illness as white structures that are shown in Figure 3. The T1-weighted MR image provide soft tissue information in a clearer way, but it is unable to detect abnormalities present in the image. The MRA image can easily detect abnormalities but not soft tissue information because of low spatial resolution. Hence, the fusion of these two images gives complementary information in a single image, which can be helpful for better medical diagnostics. Figure 3(H) gives the fused image for the proposed method and in comparison with the existing methods the proposed method fused image has high spatial resolution. From Table 2 proposed method has better values of quality metrics such as pixel intensity since they are calculated for a wider range of output pixels than do the other existing fusion methods, and this completely eliminates vagueness from the input source images. MR and MRA images are also fused with IVIFS method and found better enhancement of illness in the fused image of Figure 3 (I). The edges transformation ($Q^{AB/F}$) of the source images are more transferred to the fused image than the proposed method fused image and it takes a value of 0.717 with less computation time of 2.48 seconds.

The third example addresses the MRI and PET images shown in Figure 4, which are taken from the Harvard University website (www.med.harvard.edu). In this paper, the MRI image is registered to the corresponding PET image, and both images are gray colored. The MRI image gives the anatomy of brain tissues and does not have functional information, but the PET image specifies the brain function and has a low spatial resolution. Fusing these two images, we obtain both extra functional information and extra spatial characteristics with no spatial distortion in the fused image, which can be observed in Figure 4(H) for the proposed method. The fused image provides complete information about the size of the disease present, that cannot be visible in other fused images and which can be better diagnosed by doctors even though the computation time is large. Table 3 briefly presents the objective criteria in comparing with all the fusion methods for MRI and PET medical data sets. Here, MRI and PET images are also fused with IVIFS method, but found less information content regarding the clarity and size of tumor present in the fused

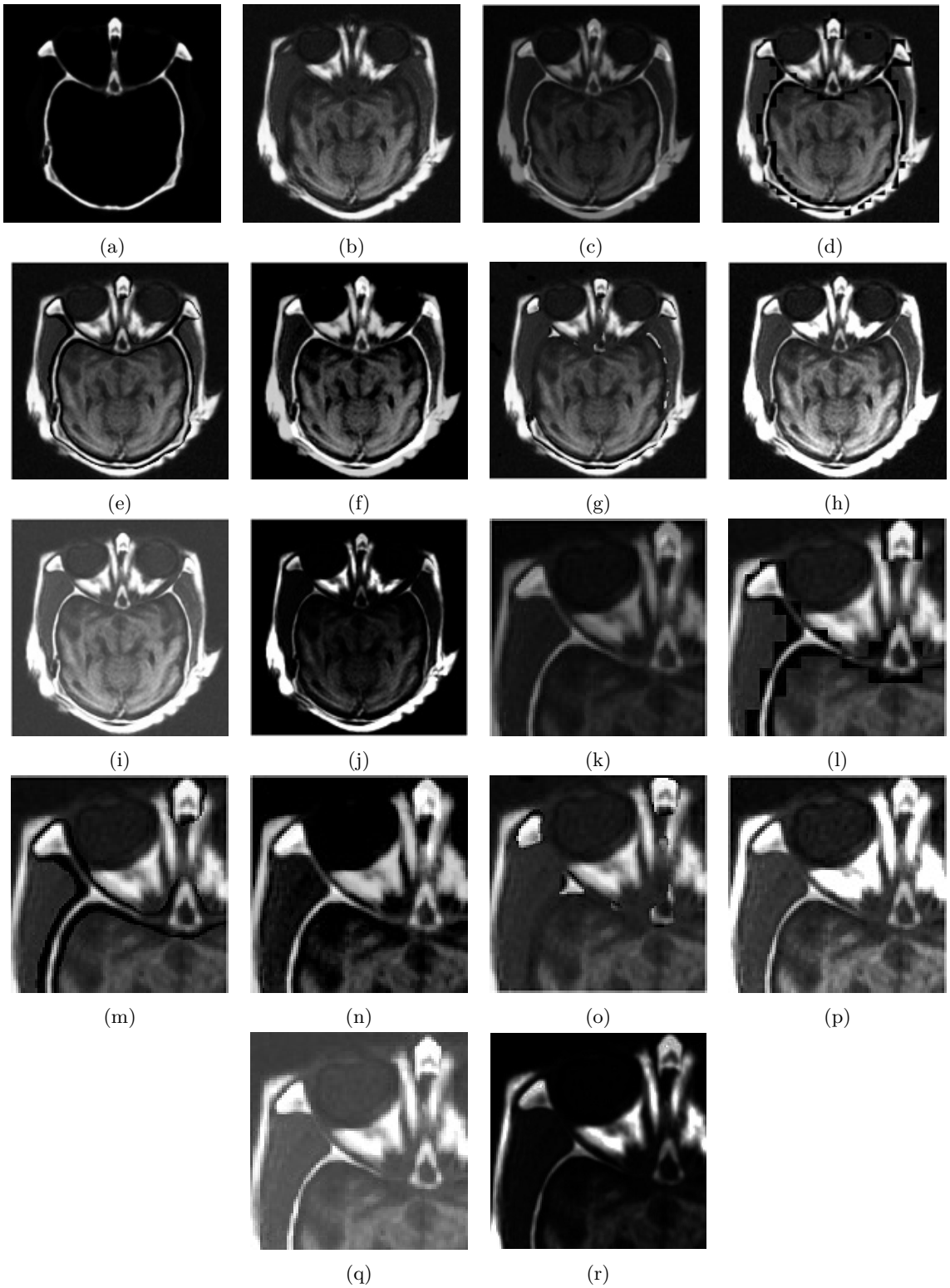

Figure 2: Fusion results for CT and MRI images. (A) CT image (B) MRI image (C) Fused image by simple average (D) Fused image by DCT (E) Fused image by RWT (F) Fused image by Intuitionistic fuzzy set (G) Fused image by Fuzzy transform (H) Fused image by proposed method (I) Fused image by Interval-valued intuitionistic fuzzy set (J) Fused image using Yue Entropy [38] (K), (L), (M), (N), (O), (P), (Q), (R) are the magnified results of (C), (D), (E), (F), (G), (H), (I) and (J) respectively.

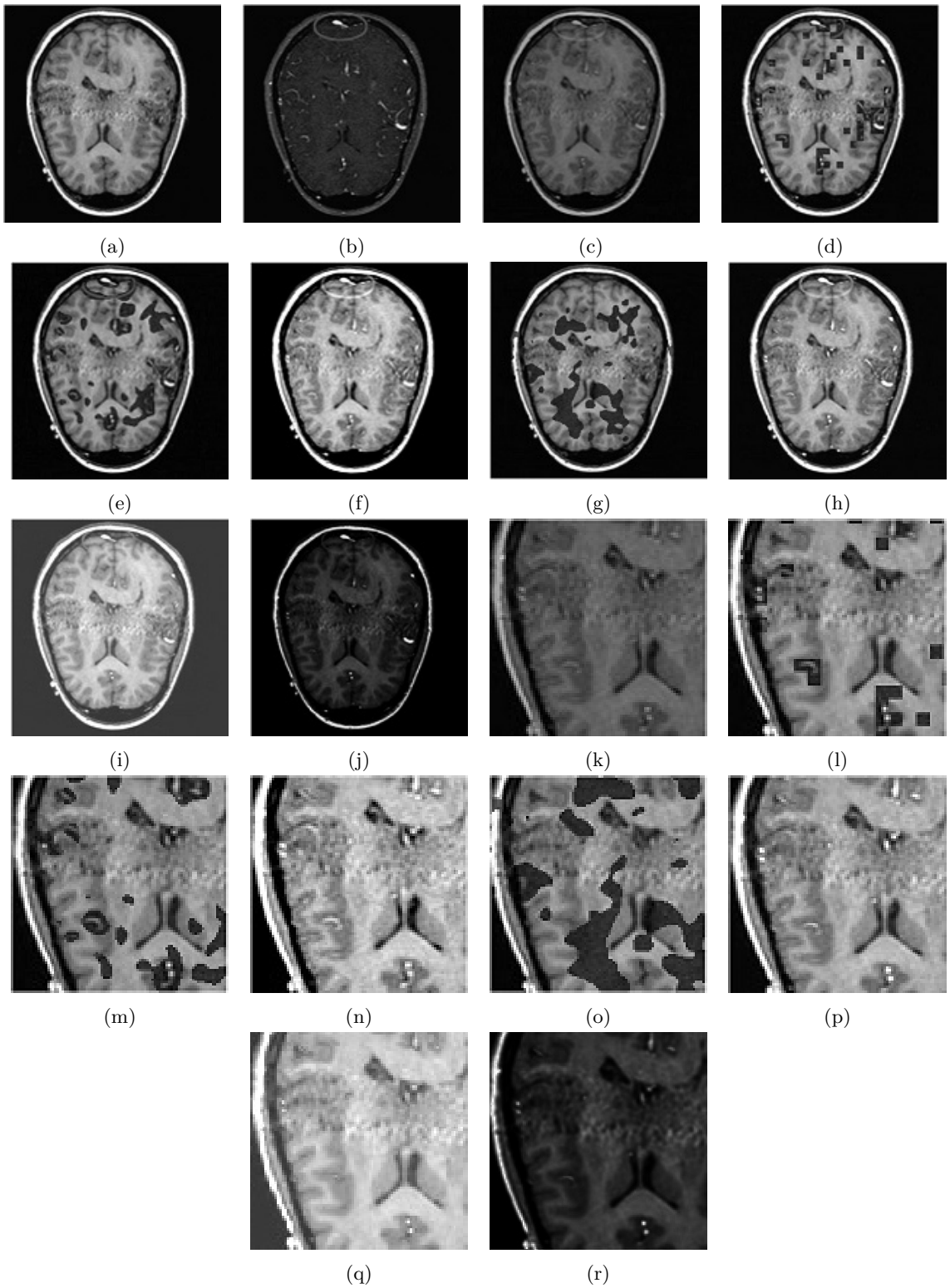

Figure 3: Fusion results for T1-weighted MR and MRA images. (A) T1-MR image (B) T1-MRA image (C) Fused image by simple average (D) Fused image by DCT (E) Fused image by RWT (F) Fused image by Intuitionistic fuzzy set (G) Fused image by Fuzzy transform (H) Fused image by proposed method (I) Fused image by Interval-valued intuitionistic fuzzy set (J) Fused image using Yue Entropy [38] (K), (L), (M), (N), (O), (P), (Q), (R) are the magnified results of (C), (D), (E), (F), (G), (H), (I) and (J) respectively.

Fusion Method	SD	AG	E	FS	CC	SF	$Q^{AB/F}$	CoT
Naidu et al.[28]	47.04	11.16	5.610	1.924	0.997	26.10	0.621	2.04
Haghighat et al.[16]	67.91	16.59	6.073	1.874	0.968	32.93	0.757	3.65
Li et al.[22]	67.06	17.48	6.196	1.903	0.947	33.83	0.747	5.07
Bala et al.[5]	86.36	17.57	5.17	1.936	1	35.85	0.641	4.23
Meenu et al.[26]	64.63	16.78	6.065	1.898	0.924	33.57	0.704	2.96
Proposed method	76.12	16.32	5.956	1.930	1	33.12	0.710	4.02
IVIFS method	64.94	13.27	5.704	1.888	1	26.63	0.717	2.48

Table 2: Objective evaluation of different image fusion methods with proposed Yager's intuitionistic fuzzy complement set method for Figure 3

Fusion Method	SD	AG	E	FS	CC	SF	$Q^{AB/F}$	CoT
Naidu et al.[28]	46.52	11.43	3.956	1.922	0.851	35.30	0.619	2.09
Haghighat et al.[16]	58.41	18.49	4.110	1.902	0.788	44.35	0.765	3.25
Li et al.[22]	53.77	18.09	4.054	1.917	0.788	43.66	0.761	4.94
Bala et al.[5]	71.46	18.97	3.928	1.933	0.822	44.51	0.729	4.04
Meenu et al.[26]	55.10	13.48	3.543	1.942	0.790	40.20	0.598	2.89
Proposed method	72.60	18.96	4.406	1.941	0.833	43.53	0.743	4.34
IVIFS method	58.61	15.66	4.316	1.924	0.830	37.87	0.748	2.97

Table 3: Objective evaluation of different image fusion methods with proposed Yager's intuitionistic fuzzy complement set method for Figure 4

Fusion Method	SD	AG	E	FS	CC	SF	$Q^{AB/F}$	CoT
Naidu et al.[28]	32.40	10.68	3.773	1.713	0.655	33.51	0.632	2.83
Haghighat et al.[16]	35.49	16.99	4.245	1.656	0.575	37.95	0.790	3.20
Li et al.[22]	35.52	17.08	4.212	1.657	0.580	38.03	0.793	4.80
Bala et al.[5]	32.07	5.620	0.979	1.826	0.475	32.60	0.474	3.89
Meenu et al.[26]	32.56	6.050	1.400	1.736	0.578	32.64	0.499	2.84
Proposed method	34.81	14.62	4.181	1.752	0.656	36.07	0.754	3.77
IVIFS method	30.89	16.77	4.765	1.685	0.628	34.20	0.787	2.92

Table 4: Objective evaluation of different image fusion methods with proposed Yager's intuitionistic fuzzy complement set method for Figure 5

image of Figure 4 (I). Figures 3(K-R) represent the magnified results of the fused images of 3(C-J) and can be readily certain that the tumor is enhanced properly in the bottom side of the magnified figures.

The fourth set of images are MRI and SPECT brain tumor images of magnitude taken from the Harvard University website (www.med.harvard.edu), and they are shown in Figure 5 for the evaluation of different fusion algorithms. It can be observed that from the MRI image, we obtain anatomical information, while the SPECT image gives physiological/functional knowledge of the human brain. To have both types of knowledge simultaneously, the images are to be fused. Figure 5(H) show the fused image by the proposed method, and the tumor is clearly enhanced when compared with other existing methods. It is clearly observed that high accuracy is attained by the proposed method efficiently abstracts the complementary and redundant information from MRI and SPECT images thereby producing a extremely consistent fused output image for detection of the tumor. Table 4 provides superiority of proposed method in terms of average number of bits per pixel, standard deviation and spatial frequency.

The last example addresses X-ray and VA (vibro-acoustography) images as shown in Figure 6. The registered X-ray and VA images provide complimentary information about breast. The schematic diagram of combined vibro-acoustography-mammography system used for the image generation is available in [2] where X-ray images are generated by Mammotest/Mammovision (Fischer Imaging Corporation's HF-X Mammography) arrangement furnished with compression racket to restrain the target (breast). Vibro-acoustography transducer is mounted in a water tank devoted to the mammography system. The X-ray image does not provide information about the deepness or thickness of the disease object, whereas VA, on the other hand, is not hampered by tissue density. VA is a new imaging modality that

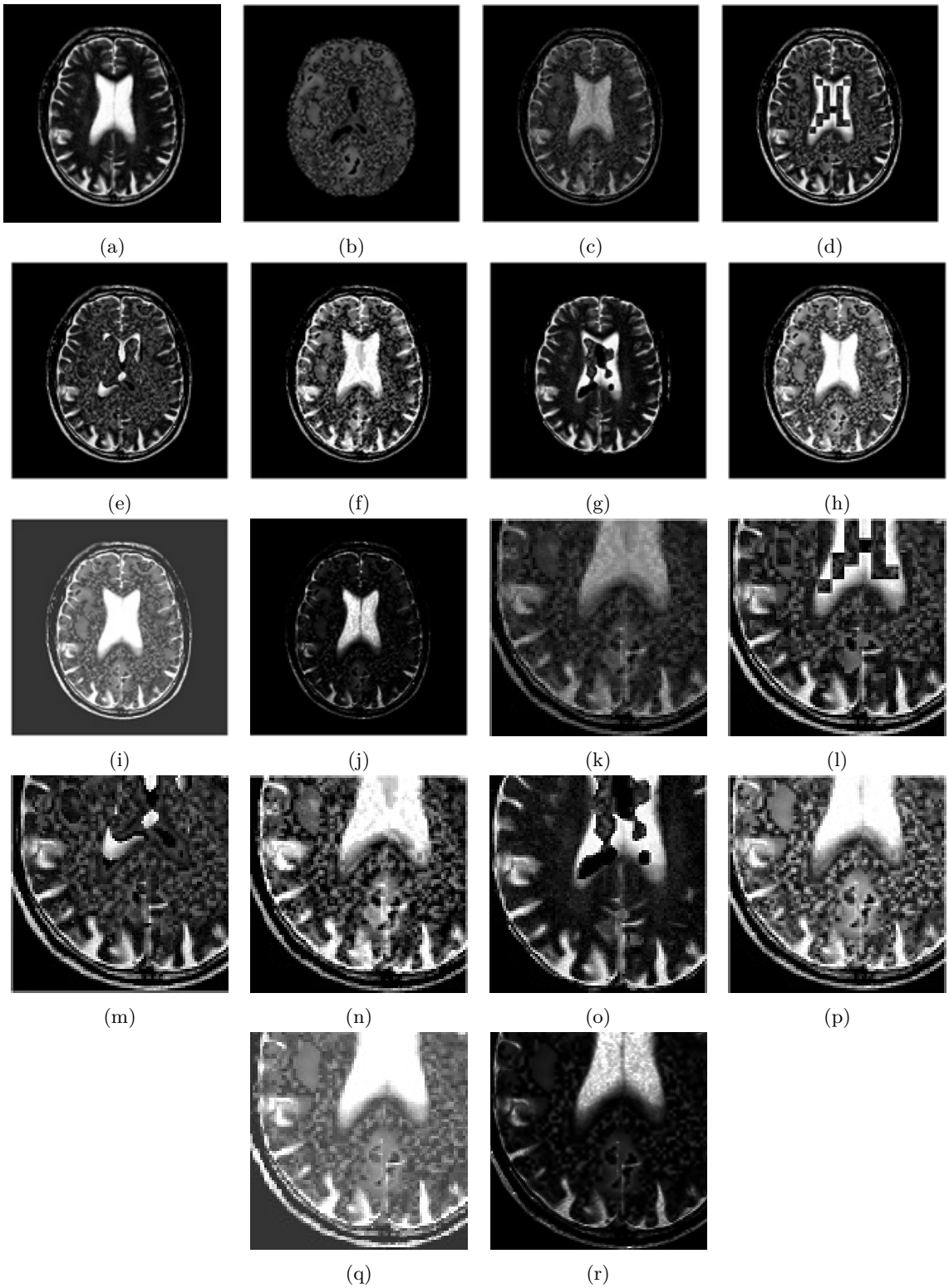

Figure 4: Fusion results for MRI and PET images. (A) MRI image (B) PET image (C) Fused image by simple average (D) Fused image by DCT (E) Fused image by RWT (F) Fused image by Intuitionistic fuzzy set (G) Fused image by Fuzzy transform (H) Fused image by proposed method (I) Fused image by Interval-valued intuitionistic fuzzy set (J) Fused image using Yue Entropy [38] (K), (L), (M), (N), (O), (P), (Q), (R) are the magnified results of (C), (D), (E), (F), (G), (H), (I) and (J) respectively.

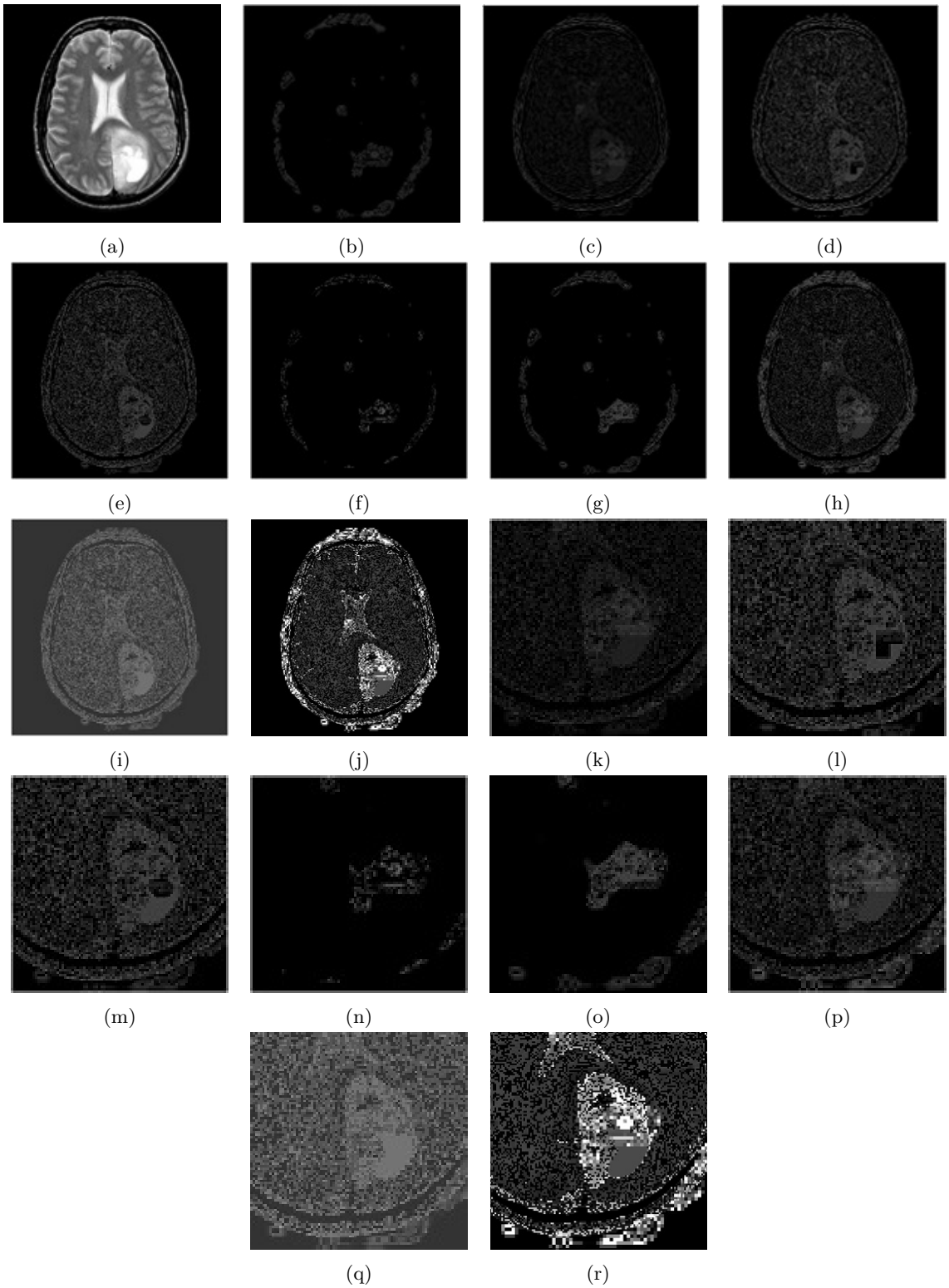

Figure 5: Fusion results for MRI and SPECT images. (A) MRI image (B) SPECT image (C) Fused image by simple average (D) Fused image by DCT (E) Fused image by RWT (F) Fused image by Intuitionistic fuzzy set (G) Fused image by Fuzzy transform (H) Fused image by proposed method (I) Fused image by Interval-valued intuitionistic fuzzy set (J) Fused image using Yue Entropy [38] (K), (L), (M), (N), (O), (P), (Q), (R) are the magnified results of (C), (D), (E), (F), (G), (H), (I) and (J) respectively.

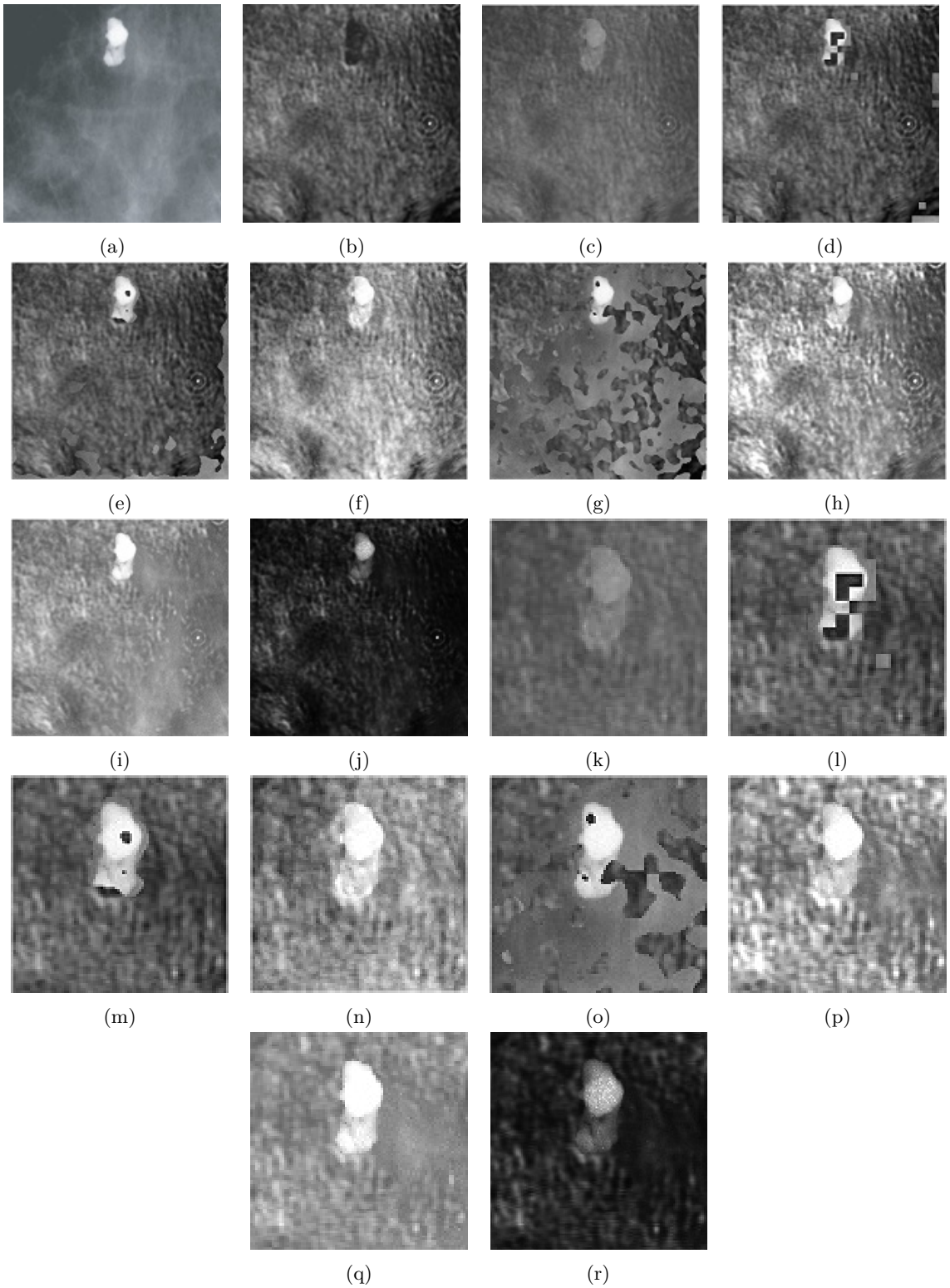

Figure 6: Fusion results for X-ray and VA images. (A) X-ray image (B) VA image (C) Fused image by simple average (D) Fused image by DCT (E) Fused image by RWT (F) Fused image by Intuitionistic fuzzy set (G) Fused image by Fuzzy transform (H) Fused image by proposed method (I) Fused image by Interval-valued intuitionistic fuzzy set (J) Fused image using Yue Entropy [38] (K), (L), (M), (N), (O), (P), (Q), (R) are the magnified results of (C), (D), (E), (F), (G), (H), (I) and (J) respectively.

Fusion Method	SD	AG	E	FS	CC	SF	$Q^{AB/F}$	CoT
Naidu et al.[28]	20.48	7.484	5.966	1.944	0.759	16.16	0.513	2.10
Haghighat et al.[16]	32.58	12.02	6.830	1.662	0.671	20.21	0.801	3.37
Li et al.[22]	31.35	12.08	6.810	1.663	0.651	20.29	0.738	6.81
Bala et al.[5]	42.86	15.44	7.400	1.999	0.788	21.00	0.700	5.14
Meenu et al.[26]	34.33	13.32	6.936	1.989	0.636	23.90	0.474	2.92
Proposed method	42.78	16.36	7.345	1.714	0.711	21.64	0.639	4.08
IVIFS method	25.91	10.15	6.455	1.886	0.675	14.58	0.658	2.98

Table 5: Objective evaluation of different image fusion methods with proposed Yager's intuitionistic fuzzy complement set method for Figure 6

is based on ultrasound stimulated acoustic emission that can be unified with X-ray to increase breast cancer diagnosis. Thus, by fusing two images, the diagnostic values of two modality images will be more than individual images, so that more information regarding the X-ray and VA can be observed in [18]. The fused image for the proposed method can be observed in Figure 6(H), which provide more information content than do the other existing methods. Table 5 gives a comparison regarding the quality metrics.

6 Conclusions

This paper grants a new method for fusing multimodal medical images using Yager's intuitionistic fuzzy complement set. The proposed algorithm is tested on several pairs of medical images, and it is found that the proposed method gives improved visual and quantitative results, with high contrast and luminance. Better results are obtained using YIFCS because it considers a greater number of uncertainties and incorporates a hesitation degree. As medical images are a low contrast with vague regions and boundaries, IFS aids in solving these problems. This algorithm is also included with intuitionistic fuzzy entropy to optimize the best parameter for membership, non-membership and hesitation degree functions. Further work includes the usage of neuro-fuzzy logic for improved image quality.

References

[1] B. S. Abdul, M. Arfanjaffar, A. Hussain, M. M. Anwar, *Block based pixel level multi-focus image fusion using particle swarm optimization*, International Journal of Innovative Computing, Information and Control, **7(7A)**(2011), 3583-3596.

[2] A. Alizad, D. H. Whaley, J. F. Greenleaf, M. Fatemi, *Potential applications of vibro-acoustography in breast imaging*, Technology in Cancer Research and Treatment, **4(2)**(2005), 151-157.

[3] K. Atanassov, *Intuitionistic fuzzy sets*, Fuzzy Sets and Systems, **20(1)**(1986), 87-96.

[4] K. Atanassov, G. Gargov, *Interval valued intuitionistic fuzzy sets*, Fuzzy Sets and Systems, **31(3)**(1989), 343-349.

[5] P. Balasubramaniam, V. P. Ananthi, *Image fusion using intuitionistic fuzzy sets*, Information Fusion, **20**(2014), 21-30.

[6] K. G. Baum, K. Raerty, M. Helguera and E. Schmidt, *Investigation of PET/MRI image fusion schemes for enhanced breast cancer diagnosis*, IEEE Conference on Nuclear Science Symposium (NSS), October 28-November 3, Honolulu, Hawaii, **5**(2007), 3774-3780.

[7] G. Bhatnagar, Q. Wu and Z. Liu, *Directive contrast based multimodal medical image fusion in NSCT domain*, IEEE Transactions on Multimedia, **15(5)**(2013), 1014-1024.

[8] C. Bhuvaneswari, P. Aruna, D. Loganathan, *A new fusion model for classification of the lung diseases using genetic algorithm*, Egyptian Informatics Journal, **2**(2014), 69-77.

[9] P. Burillo, H. Bustince, *Entropy on intuitionistic fuzzy set and on interval-valued fuzzy set*, Fuzzy Sets and Systems, **78**(1996), 305-316.

[10] H. Bustince, J. Kacpryzk, V. Mohedano, *Intuitionistic fuzzy generators: application to intuitionistic fuzzy complementation*, Fuzzy Sets and Systems, **114**(2000), 485-504.

[11] T. Chaira, *A novel intuitionistic fuzzy c means clustering algorithm and its application to medical images*, Applied Soft Computing, **11(2)**(2011), 1711-1717.

[12] S. Das, M. K. Kundu, *Ripplet based multimodality medical image fusion using pulse-coupled neural network and modified spatial frequency*, IEEE International Conference on Recent Trends in Information Systems, December 21-23, Kolkata, India, (2011), 229-234.

[13] L. A. De, S. Termni, *A definition of non-probabilistic entropy in the setting of fuzzy set theory*, Information Control, **20(4)**(1972), 301-312.

[14] W. Dou, S. Ruan, Y. Chen, D. Bloyet, J. M. Constans, *A framework of fuzzy information fusion for the segmentation of brain tumour tissues on MR images*, Image and Vision Computing, **25(2)**(2007), 164-171.

[15] E. Z. A. E. G. Fatma, E. Mohammed, A. Ahmed, *Current trends in medical image registration and fusion*, Egyptian Informatics Journal, **17(1)**(2016), 99-124.

[16] M. B. A. Haghighat, A. Aghagolzadeh, H. Seyedarabi, *Multi-focus image fusion for visual sensor networks in DCT domain*, Computers and Electrical Engineering, **37(5)**(2011), 789-797.

[17] C. He, Q. Liu, H. Li, H. Wang, *Multimodal medical image fusion based on IHS and PCA. Procedia Engineering*, Symposium on Security Detection and Information Processing, November 12-14, Hefei, China, **7**(2010), 280-285.

[18] H. G. Hosseini, A. Alizad, M. Fatemi, *Integration of Vibro-Acoustography imaging modality with the traditional mammography*, International Journal of Biomedical Imaging, **2007**(2007), 1-8.

[19] P. Jagalingam, A. V. Hegde, *A Review of quality metrics for fused image*, Aquatic Procedia, International Conference on Water Resources, Coastal and Ocean Engineering (ICWRCOE), March 12-14, Mangalore, Karnataka, India, **4**(2015), 133-142.

[20] A. P. James, B. V. Dasarathy, *Medical image fusion: a survey of the state of the art*, Information Fusion, **19**(2014), 4-19.

[21] I. Kaplan, E. Kolupka, M. Morrissey, *MRI-ultrasound image fusion for 125I prostate implant treatment planning*, International Journal of Radiation Oncology Biology Physics, **42(1)**(1998), 294.

[22] X. Li, M. He and M. Roux, *Multifocus image fusion based on redundant wavelet transform*, IET Image Processing, **4(4)**(2010), 283-293.

[23] S. Li, X. Kang, L. Fang, *Pixel-level image fusion: A survey of the state of the art*, Information Fusion, **33(C)**(2017), 100-112.

[24] H. Li, B. S. Manjunath, S. K. Mitra, *Multisensor image fusion using the wavelet transform*, Graph Models Image Process, **57(3)**(1995), 235-245.

[25] J. Liang, Y. He, D. Liu and X. Zeng, *Image fusion using higher order singular value decomposition*, IEEE Transactions on Image Processing **21(5)**(2012), 2898-2909.

[26] M. Meenu, S. Rajiv, *A novel method of multimodal medical image fusion using fuzzy transform*, Journal of Visual Communication and Image Representation, **40**(2016), 197-217.

[27] H. O. S. Mishra, S. Bhatnagar, *MRI and CT image fusion based on wavelet transform*, International Journal of Information and Computation Technology, **4(1)**(2014), 47-52.

[28] V. P. S. Naidu, J. R. Raol, *Pixel level image fusion using wavelets and principal component analysis*, Defense Science Journal, **58(3)**(2008), 338-352.

[29] B. K. Shreyamshakumar, *Multifocus and multispectral image fusion based on pixel significance using discrete cosine harmonic wavelet transform*, Signal, Image and Video Processing, **7(6)**(2013), 1125-1143.

[30] E. Szmidt, J. Kacpryzyk, *Distance between intuitionistic fuzzy set*, Fuzzy Sets Systems, **114(3)**(2000), 505-518.

[31] Z. Tanish, Z. Mukesh, *A Novel region based multimodality image fusion method*, Journal of Pattern Recognition Research, **6(2)**(2011), 140-153.

[32] A. Toet, J. J. Vanruyven, J. M. Valeton, *Merging thermal and visual images by a contrast pyramid*, Optical Engineering, **28(7)**(1989), 789-792.

[33] Y. Wu, C. Wang, S. C. Ng, A. Madabhusi, Y. Zhong, *Breast cancer diagnosis using neural-based linear fusion strategies*, Processing of Springer, International Conference on Neural Information Processing (ICONIP)., October 3-6, Hong Kong, China, (2006), 165-175.

[34] R. R. Yager, *Some aspects of intuitionistic fuzzy sets*, Fuzzy Optimization and Decision Making, **8(1)**(2009), 67-90.

[35] Y. Yang, D. S. Park, S. Huang, N. Rao, *Medical image fusion via an effective wavelet based approach*, EURASIP Journal on Advances in Signal Processing, **2010**(2010), 1-13.

[36] Z. L. Yue, *A group decision making approach based on aggregating interval data into interval-valued intuitionistic fuzzy information*, Applied Mathematical Modelling, **38(2)**(2014), 683-698.

[37] C. Yue, *A geometric approach for ranking interval-valued intuitionistic fuzzy numbers with an application to group decision-making*, Computers & Industrial Engineering, **102**(2016), 233-245.

[38] C. Yue, *Entropy-based weights on decision makers in group decision-making setting with hybrid preference representations*, Applied Soft Computing, **60**(2017), 737-749.

[39] L. A. Zadeh, *Fuzzy sets*, Information Control, **8(3)**(1965), 338-353.

MULTIMODAL MEDICAL IMAGE FUSION BASED ON YAGER'S INTUITIONISTIC FUZZY SETS

T. TIRUPAL, B. CHANDRA MOHAN AND S. SRINIVAS KUMAR

ترکیب تصویر طبی چند کیفیتی بر اساس مجموعه‌های فازی شهودی یاگر(Yager)

چکیده. هدف از ترکیب تصویر برای تصاویرطبی ترکیب تصاویر چندگانه بدست آمده از منابع مختلف دریک تصویر مناسب برای تشخیص-های بهتر می‌باشد. مطابق آخرین پیشرفت‌های علمی تکنیک ترکیب تصویر بر اساس مجموعه‌های غیر–فازی است، و چنین تصویر ترکیبی بدست آمده نسبت به اطلاعات تکمیلی دارای تأخیر است. مجموعه‌های فازی شهودی (IFS) برای غیرنظامی مناسب‌تر است و پردازش تصویر طبی به عنوان عدم قطعیت‌های بیشتر برای مقایسه با نظریه مجموعه فازی در نظر گرفته می‌شوند.

دراین مقاله، برای ترکیب مؤثر تصاویر طبی چند کیفیتی یک الگوریتم ارائه گردیده‌است. در روش پیشنهادی، ابتدا تصاویر به تصاویر مکمل فازی شهودی یاگر (Yager) (YIFCIs) تبدیل می شود، و یک تابع هدف جدید، که انتروپی فازی شهودی (IFE) نامیده می‌شود. برای بدست آوردن مقدار بهینه پارامتر عضویت و توابع غیرعضویت به کار گرفته می‌شود. سپس، با به کار بردن مغایرت میدان دید (CV) برای ساختن یک نگاشت تصمیم (DM) ، YIFCI ها مقایسه می‌شوند. برای خلق یک تصویر ترکیبی DM با بازبینی پایداری دوباره پالایش می-شود. شبیه‌سازی‌ها روی جفت‌های متعدد از تصاویر طبی چند کیفیتی اجرا می‌شوند و با روش‌های ترکیبی موجود مانند میانگین ساده، تبدیل کسینوس گسسته (DCT)، تبدیل طول موج آزاد (RWT)، مجموعه فازی شهودی، تبدیل فازی و مجموعه‌ی فازی شهودی بازه – مقدار (IVIFS) مقایسه می‌شوند. ارجحیت روش پیشنهادی ارائه و توجیه شده‌است. کیفیت تصویر ترکیبی با متریک‌های کیفیت متعددی، مانند فراوانی خاص (FS) ، گرادیان میانگین (AG) ، تقارن ترکیب (FS)، حفظ اطلاعات یالی ($Q^{AB/F}$)، انتروپی (E) و زمان محاسبه (CoT) تأیید شده است.